Int. J. Multiphase Flow Vol. 19, No. 1, pp. 27–34, 1993
Printed in Great Britain

0301-9322/93 $6.00 + 0.00
Pergamon Press Ltd

THE EFFECT OF PRESSURE ON THE PHASE TRANSITION FROM BUBBLING TO TURBULENT FLUIDIZATION

M. TSUKADA, D. NAKANISHI and M. HORIO
Department of Chemical Engineering, Tokyo University of Agriculture and Technology, Koganei, Tokyo 184, Japan

(Received 2 July 1991; in revised form 2 October 1992)

Abstract—Bubbling, turbulent and fast fluidized beds are the major phases of gas–solid dense suspensions. In this paper the effect of pressure on the phase transition from bubbling to turbulent fluidization was investigated over the pressure range 0.1–0.7 MPa with a small-scale circulating fluidized bed placed in a pressure vessel. It has been found that the gas velocity at which the transition takes place decreases with increasing pressure but the solid mass flux at the transition remains almost constant. Detailed measurements on the meso-scale flow structures were made to explain the transition characteristics.

Key Words: gas–solid fluidization, phase transition, bubbling, turbulent, pressurized circulating fluidized bed

INTRODUCTION

Pressurized circulating fluidized beds are expected to have advantages common to both pressurized fluidized beds and circulating fluidized beds. Pressurized fluidized beds are more compact than atmospheric fluidized beds of the same gas throughput. With increasing pressure, the heat transfer coefficient between the bed and immersed surfaces becomes higher. Circulating fluidized beds have a number of advantages, including highly efficient solid retention and the capabilities of wide turn down and the handling of cohesive materials.

Pressurized circulating fluidized beds are now to be applied to coal combustion boilers, whose pressure is expected to be up to 1.6 MPa. Applications to catalytic reactions have also been attempted, whose pressure is much higher than the boilers'—reaching 8 MPa in some cases. Pressurized circulating fluidized beds would also be advantageous for reactors to treat heavy and cohesive particles, because of the high pneumatic transport capability of pressurized gas. In spite of these advantages, fundamental studies of pressurized circulating fluidized beds are relatively new and only a few works have been reported.

Concerning atmospheric circulating fluidized beds, hydrodynamic studies have been conducted intensively during the last 5 years. The essential hydrodynamic structure of circulating fluidized beds, including the axial voidage distribution, the annular flow structure and the clustering behavior, is becoming clearer. Among the hydrodynamic issues, the phase transitions of bubbling to turbulent and turbulent to fast fluidization are quite significant since essential changes in the structure of the dense suspensions take place following these transitions, as discussed by Horio (1991). Furthermore, phase transitions are important since the fundamental rate parameters for reactor design and operation change in accordance with the flow regimes of fluidization. However, the behavior of such particle suspensions has not been well-formulated, even in atmospheric conditions.

Historically, the hydrodynamic study of pressurized fluidized beds at a gas velocity higher than the ordinary bubbling fluidization was initiated by Lanneau (1960), who measured the local density fluctuations of the FCC (fluidized cracking catalyst) bed by a capacitance probe under 0.17 and 0.52 MPa.

Canada & McLaughlin (1978) measured the bubbling to turbulent phase transition in beds of coarse particles of 0.65 and 2.0 mm dia under pressures of up to 1 MPa, and observed no remarkable change in the transition superficial gas velocity in different pressure beds.

Using a γ-ray densitometer, Weimer & Jacob (1986) measured the bed density fluctuation in a turbulent fluidized bed of 97 mm i.d. under pressure elevations of up to 6.2 MPa. They reported

that they did *not* observe a sudden decrease in the pressure fluctuation during the bubbling to turbulent phase transition with an increasing superficial gas velocity under high-pressure conditions.

Yang & Chitester (1988) measured the gas velocity of the bubbling to turbulent transition by visual observations with a two-dimensional bed of various particle species up to 6.4 MPa and compared their experimental values with those calculated from the correlation developed using atmospheric data.

Hashimoto (1989; Hashimoto *et al.* 1988) determined the onset velocity of turbulent fluidization, u_k, via the pressure fluctuation in a hot bench-scale pressurized fluidized bed of catalyst particles.

Horio *et al.* (1992) measured the offset velocity of bubbling fluidization, u_c, as well as the onset velocity of turbulent fluidization, u_k, for FCC and silica sand under ambient conditions.

Ishii & Murakami (1991) measured u_c and u_k for FCC under ambient conditions for two geometrically similar rigs.

Tsukada *et al.* (1991) plotted their data on the Re (Reynolds number) vs Ar (Archimedes number) plane with data in the literature. Data have been also compared with Horio's (1986; Horio & Morishita 1988) correlations for u_c and u_k. It has been found that the Reynolds number data (Re_c and Re_k corresponding to the transition velocities u_c and u_k, respectively) from pressurized fluidized beds are slightly smaller than those from atmospheric beds.

However, it must be noted here that no systematic data have been presented with respect to the phase transition characteristics with sufficient specification of the circulating flux, the longitudinal voidage distributions and the meso-scale bed structures, which can be observed from fluctuations of local voidage and pressure.

The objective of the present work is to investigate the effect of pressure on the transition from bubbling to turbulent fluidization based on the meso-scale flow structure measurements.

EXPERIMENTAL APPARATUS AND METHOD

A laboratory-scale circulating fluidized bed (50 mm i.d., 400 mm high) with a filter canvas distributor was located in a pressure vessel. Schematics of the fluidized bed and the measurement system are shown in figure 1. Pressure transducers and load cells were located inside the vessel. Electrical signals passed through flanges; optical signals were taken through optical fibers out of the vessel. The solid circulating rate was controlled by a butterfly valve. After the pressure in the vessel reached a specified value, the flow rate in the column and the downcomer were adjusted to the specified value.

The axial pressure distribution and the pressure fluctuation were measured with semiconductor pressure transducers (0–0.1 MPa) in the same manner as previously (Horio *et al.* 1989). The solid circulating rate was measured with the particle flow meter reported in Horio *et al.* (1992). The bed density fluctuation was measured in terms of the light reflection from the bed with an optical fiber probe. Pressure and bed density fluctuations were measured at a height of 80 mm from the column bottom. This height was chosen so that the measurements could always be performed in the lower density zone of the riser over the gas velocity range examined in this work. The optical fiber probe, consisting of three vertically aligned fibers of 250 μm dia (i.e. one lighting fiber at the center and two light-receiving fibers), was inserted horizontally into the center of the column.

Experiments were done using FCC particles (particle diameter, $d_p = 46.4\ \mu$m; particle density, $\rho_p = 1780\ \text{kg/m}^3$). The minimum fluidization velocity of the present powder estimated from the Wen & Yu (1966) correlation is 1 mm/s and does not change its value over the present pressure range. The operating pressures were 0.1, 0.18, 0.35 and 0.70 MPa. The superficial gas velocity for the downcomer aeration, $u_{\text{downcomer}}$, was 2.2×10^{-3} m/s at all operating pressures. The butterfly valve for controlling the solid circulation rate was always kept fully opened. The measured values of the solid circulating flux, G_s, under different pressures are shown in figure 2 as a function of the superficial gas velocity, u_0.

The sampling frequency of the light reflection signals was chosen as 500 Hz. This frequency was proved to be sufficiently high to represent the signal. The original signals were smoothed to eliminate high-frequency components, which might be related to the motion of individual particles

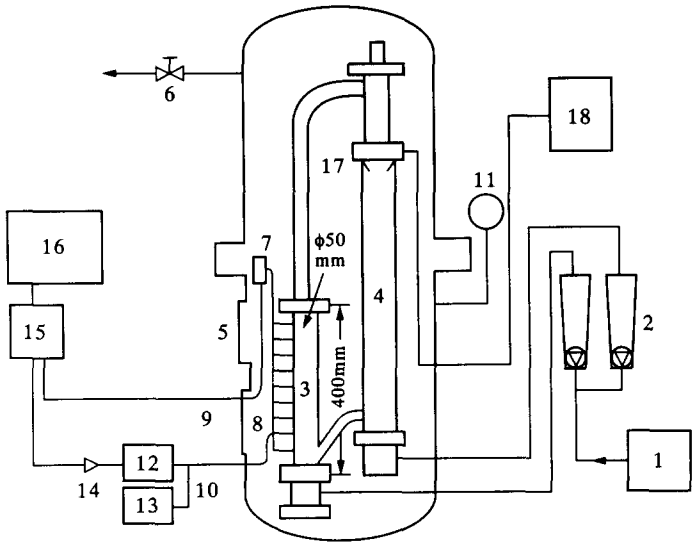

1. Compressor
2. Rotameter
3. Riser
4. Downcomer
5. View port
6. Exhaust valve
7. Pressure transducers
8. Optical fiber probe
9. Electric cable
10. Optical fiber
11. Pressure gauge
12. Photomultiplier
13. Laser
14. DC amplifier
15. A/D-converter
16. Computer
17. Solid circulation meter
18. Pen recorder

Figure 1. Schematic diagram of the pressurized circulating fluidized bed and the measuring system.

or very small groups of particles, so that the dense phase and lean phase were more clearly distinguishable. The smoothing was done by taking the arithmetic average of successive n signals over the period of $n\Delta t$. The time period of averaging, $n\Delta t$, was adjusted to 6 ms. The sampling frequency of the pressure fluctuation was set as 1000 Hz.

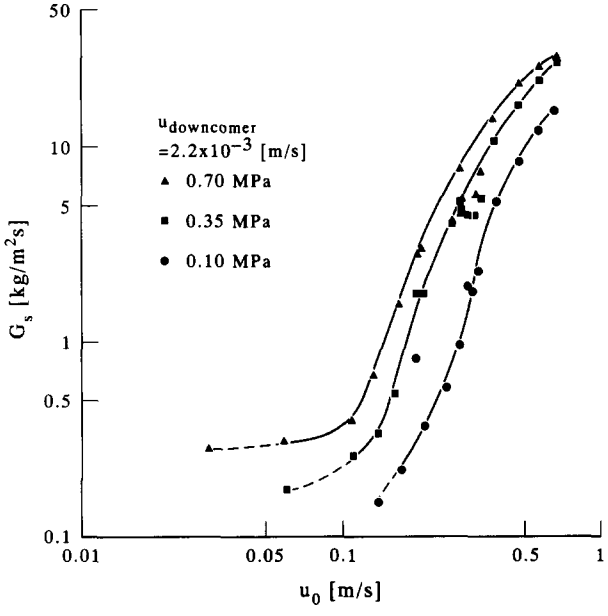

Figure 2. G_s under the present conditions.

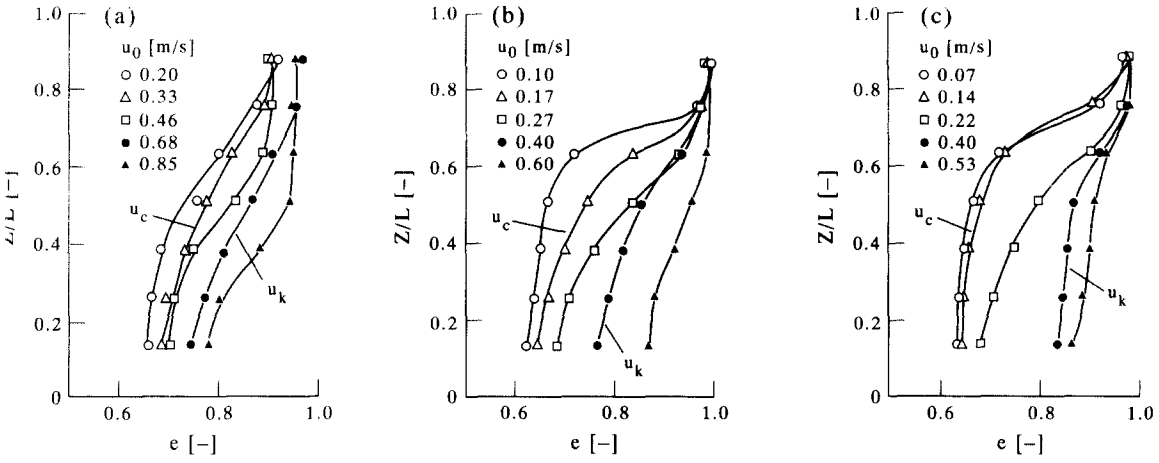

Figure 3. Axial voidage distribution under three different pressures: (a) $P = 0.10$ MPa; (b) $P = 0.35$ MPa; (c) $P = 0.70$ MPa.

RESULTS AND DISCUSSION

Figures 3 and 4 show the dependency of the axial voidage distribution and the root-mean-square pressure fluctuation, $P'_{\text{r.m.s.}}$, on the gas velocity under different pressures. From figure 3 it can be confirmed that the pressure tap was always in the dense region. From figure 4 the offset velocity of bubbling fluidization, u_c, and the onset velocity of turbulent fluidization, u_k, were determined in the same manner as by Yerushalmi & Cankurt (1979). According to their work, u_c is defined as the superficial gas velocity, u_0, at which $P'_{\text{r.m.s.}}$ shows its maximum; and u_k is the gas velocity at which $P'_{\text{r.m.s.}}$ ceases to decrease with further increases in the gas velocity. As can be seen in figure 4, both the peak value of $P'_{\text{r.m.s.}}$ and the corresponding u_c shift to lower values with increasing pressure. In figure 5, u_c and u_k are plotted against pressure; and in figure 6, $P'_{\text{r.m.s.}}$ is plotted against pressure. All of them are almost proportional to $P^{-0.3}$. One remarkable finding from this experiment is that the values G_s at both u_c and u_k are almost constant, as shown in figure 7. In addition, the axial voidage distributions at u_c or u_k are also similar under different pressures, as can be seen in figure 3.

Figure 8 shows typical signals of the light reflection intensity from one of the light-receiving fibers in terms of the reduced light reflection intensity, I, defined as

$$I = (V - V_0)/(V_1 - V_0), \qquad [1]$$

where V denotes the photomultiplier output voltage, which is proportional to the light reflection intensities from the bed, and V_0 and V_1 are those from the empty column and settled bed,

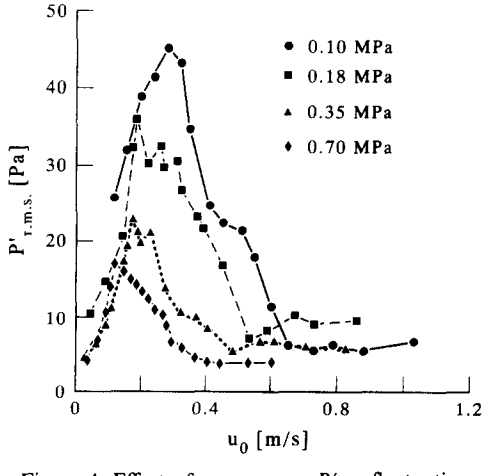

Figure 4. Effect of pressure on $P'_{\text{r.m.s.}}$ fluctuation.

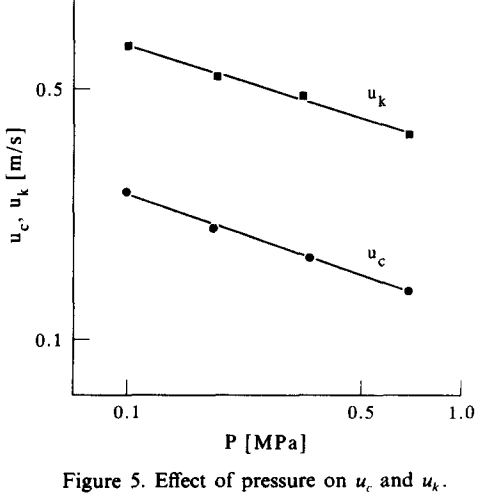

Figure 5. Effect of pressure on u_c and u_k.

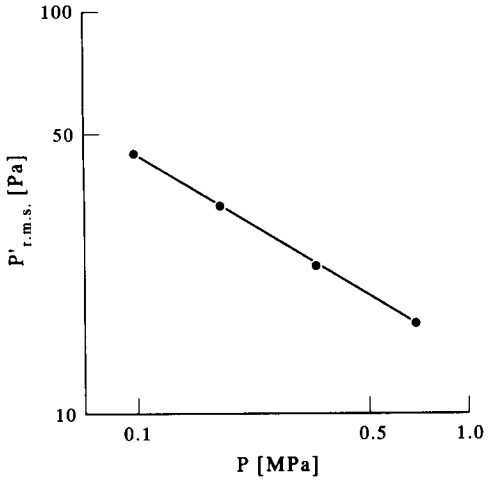

Figure 6. Effect of pressure on $P'_{r.m.s.}$ fluctuation at $u_0 = u_c$.

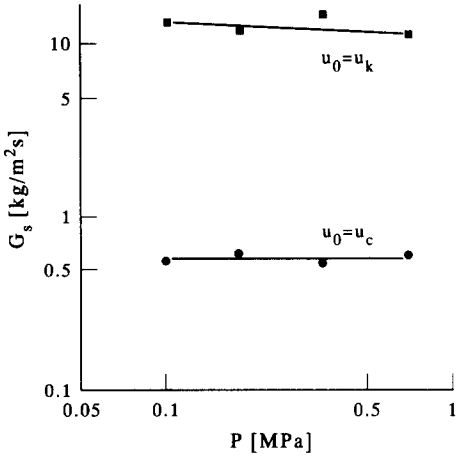

Figure 7. Effect of pressure on G_s at $u_0 = u_c$ and $u_0 = u_k$.

respectively. The unavoidable scatter in the voltage signal, which was probably caused by the random particle orientation to the probe, was smoothed by time averaging. The reflection light of intensities much higher than the value from the settled bed may be due to the vigorous impingement of solids on the probe.

The probability distributions of the light reflection are given in figure 9. Typical distributions for the clear bubbling mode show two peaks: the peak in the high reflection region corresponds to the dense phase—the reflection intensity corresponding to this peak was about unity; the other peak in the low reflection region, having a skirt wider than that of the dense phase peak, corresponds to the bubble phase which can be found around $I \simeq 0.5$—due to the scatter of the signals the skirts overlapped each other but the minimum density was found around $I = 0.8$. Accordingly, the threshold value to separate the bubble phase from the dense phase was assumed to be 0.8 for the preliminary determination of the bubble fraction, ε_b. In figure 8 the threshold value is indicated by horizontal lines.

With increasing gas velocity, the time fraction of the period during which the probe top was in the lean phase increases. The gas velocity at which the lean phase peak is formed decreases with increasing pressure, as can be seen in figure 9. This indicates that the transition from the bubbling to the turbulent regime, or to regimes of more dilute suspensions, takes place at lower gas velocities with increased pressures.

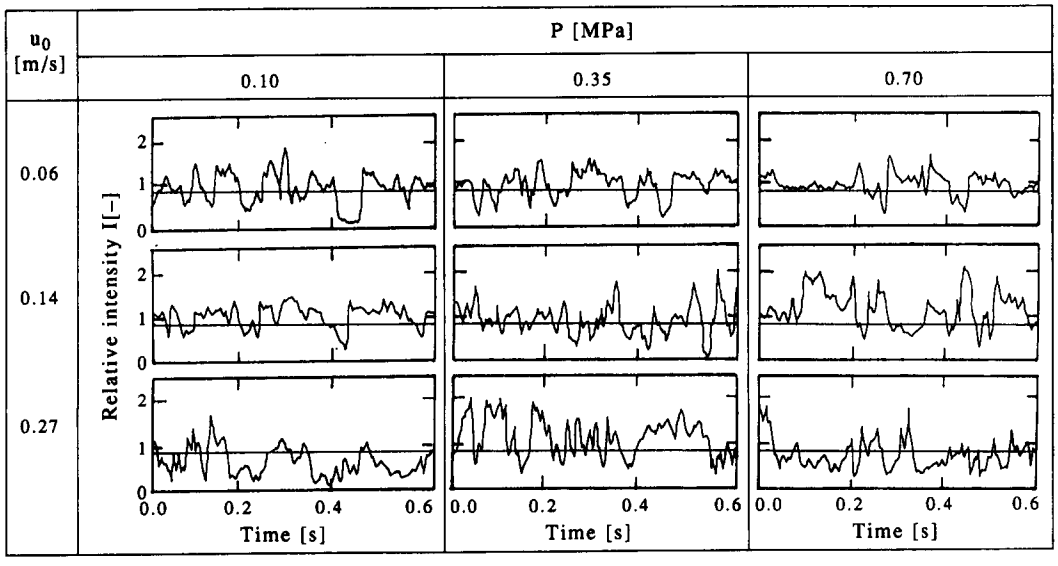

Figure 8. Examples of light reflection signals ($I = 0.8$).

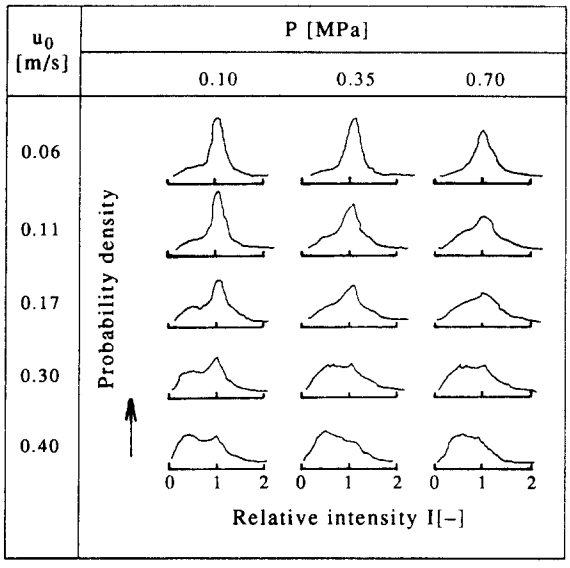

Figure 9. Probability distribution functions of light reflection signals (sample length = 32 s).

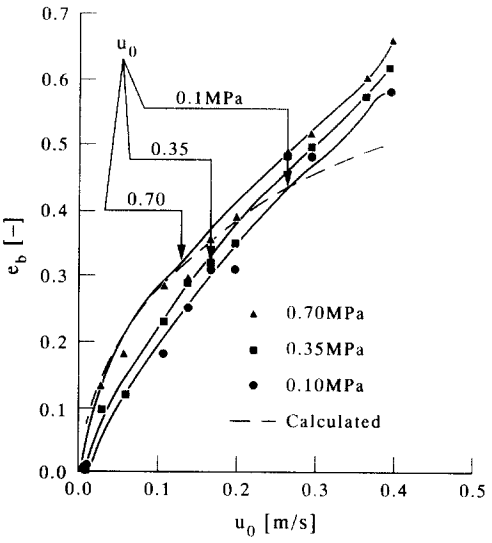

Figure 10. Effect of pressure on ε_b.

In figure 10 the bubble fraction, ε_b, is plotted against superficial gas velocity, u_0, for different pressures. This ε_b is the one formally determined as the fraction of the period during which the relative intensity of the light reflection was <0.8. As can be seen in figure 10, ε_b increased with increasing u_0, but only slightly with pressure. The value of ε_b obtained at $u_0 = u_c$ decreased from 0.4 to 0.3 and the pressure increased from 0.1 to 0.7 MPa.

In the literature, the value of ε_b can be roughly obtained from the average solid density data and the values of ε_{mf} reported by Yerushalmi & Cankurt (1979) and Avidan & Yerushalmi (1982). The value becomes $\varepsilon_b \simeq 0.46$ for their FCC ($\rho_p = 1070\,\text{kg/m}^3$, $d_p = 49\,\mu\text{m}$, $\varepsilon_{mf} = 0.45$) at $u_0 = u_c$. This value is not very different from the present data.

The bubble fraction could be a dominant factor in the bubbling to turbulent phase transition. Horio (1991) suggested that the offset of bubbling fluidization occurs when ε_b reaches an upper limit, above which bubbles can no longer exist in the bed without touching each other. From the data of Yerushalmi & Cankurt (1979), Horio (1991) estimated ε_b values taking into account the effects of bubble splitting and slug formation. The calculated values of ε_b at $u_0 = u_c$ ranged from 0.75 to 0.8, which are too high perhaps because of the weakness of the model in handling slugging behavior. The dashed curve in figure 10 shows the ε_b predicted by the same method using the equilibrium bubble diameter obtained by Horio & Nonaka (1987). The agreement is fairly reasonable, although the prediction does not include the effect of pressure. Contrary to the Yerushalmi & Cankurt (1979) conditions, no slugging was observed in the present experiments. Presumably this is why the prediction of ε_b at $u_0 = u_c$ did not present much difficulty in the present case.

To realize the image of bubble packing in the bed let us relate ε_b to the surface-to-surface pitch between the bubbles, l_b. From geometrical considerations, we have

$$l_b/D_b = \{\pi/(6\varepsilon_b)\}^{1/3} - 1 \quad \text{(for cubic packing)} \qquad [2]$$

and

$$l_b/D_b = \{\sqrt{2}\pi/(6\varepsilon_b)\}^{1/3} - 1 \quad \text{(for regular tetrahedral packing)}, \qquad [3]$$

where bubbles are assumed to be spherical. Substituting $\varepsilon_b = 0.4$, $l_b/D_b = 0.094$ is obtained for cubic packing and 0.23 for regular tetrahedral packing.

From the Clift & Grace (1971) model for bubble coalescence, the following bubble, whose diameter D_{b2} is 80% of the foregoing bubble diameter D_{b1}, will be absorbed by the foregoing bubble when the center-to-center distance between them is $<1.43\,D_{b1}$ for cubic packing and $1.25\,D_{b1}$ for regular tetrahedral packing. The distance between two bubbles at $u_0 = u_c$ obtained from the present

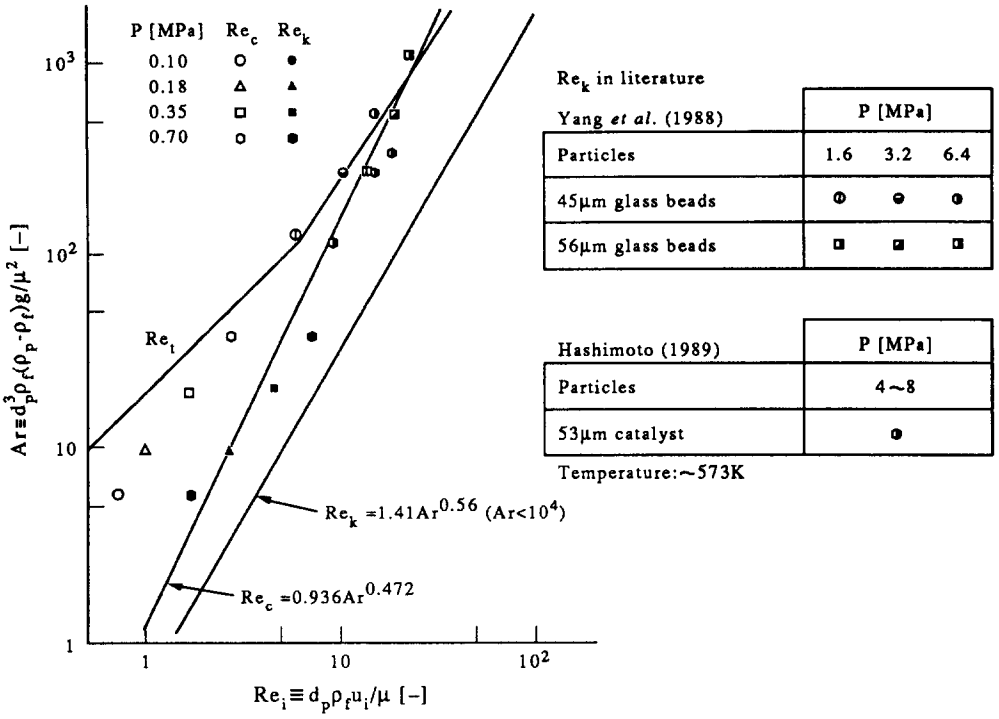

Figure 11. Transition Reynolds numbers Re_c and Re_k as functions of Ar.

experiment is sufficiently small for coalescence and presumably no bubbles can exist free from vigorous interaction.

In figure 11 the present data for u_c and u_k are compared with previous data from pressurized beds of fine particles. The pressure dependence of the present u_k data is similar to that indicated in the Yang & Chitester (1988) data. Lines show the Horio (1986; Horio & Morishita 1988) correlations for u_c and u_k, which are determined from the literature data of both atmospheric and pressurized beds. In the Horio correlations the pressure effects are taken into account in terms of the gas density, ρ_f, and viscosity, μ, in the Re and Ar. However, the prediction by the correlations showed some overestimation of the transition velocities. As already shown in the Re vs Ar plot in a previous paper (Tsukada *et al.* 1991), previous experimental data on u_c and u_k are scattered (depending on their experimental conditions and methods). Further works are necessary to describe the phase transition phenomena more systematically.

CONCLUSION

The offset velocity of bubbling fluidization, u_c, and the onset velocity of turbulent fluidization, u_k, were determined in a laboratory-scale circulating fluidized bed under different pressures up to 0.7 MPa. Both u_c and u_k for FCC particles were proportional to $P^{-0.3}$. At the conditions of each regime transition ($u_0 = u_c$ or u_k), the solid circulating flux, G_s, and the axial voidage distribution, $\varepsilon(z)$, were almost invariable irrespective of pressure. The time-to-time change of the local bed voidage, obtained with an optical fiber probe, indicated that the phase transition of bubbling to turbulent fluidization significantly changes the local bed structure. The bubble fraction determined from the probability distribution function was about 0.4 for an atmospheric bed at the offset of bubbling fluidization and decreased to 0.3 with increasing pressure up to 0.7 MPa.

Acknowledgements—The authors thank Mr A. Meio and his colleagues at Tokuju Kosakusho Co. Ltd for kindly contributing the pressure vessel.

REFERENCES

AVIDAN, A. A. & YERUSHALMI, J. 1982 Bed expansion in high velocity fluidization. *Powder Technol.* **32,** 223–232.

CANADA, G. S. & MCLAUGHLIN, M. H. 1978 Large particle fluidization and heat transfer at high pressures. *AIChE Symp. Ser.* **176**(74), 27–37.

CLIFT, R. & GRACE, J. R. 1971 Coalescence of bubbles in fluidized beds. *AIChE Symp. Ser.* **67**(116), 23–33.

HASHIMOTO, O., HARUTA, T., MOCHIZUKI, K., MATSUNAMI, W., MORI, S., HIRAOKA, S. & YAMADA, I. 1988 Criteria of transition to turbulent fluidization in the high-velocity circulating fluidized bed. *Kagaku Kogaku Ronbunshu* **14,** 309–314.

HASHIMOTO, O. 1989 Study of methanol synthesis reactor by turbulent fluidized beds. Ph.D. Thesis, Nagoya Inst. of Technology, Nagoya.

HORIO, M. 1986 High-velocity operation of fluidized beds. *J. Powder Technol. Japan* **23,** 80–90.

HORIO, M. 1991 Hydrodynamics of circulating fluidization—present status and research needs. In *Circulating Fluidized Bed Technology III* (Edited by BASU, P. *et al.*), pp. 3–14. Pergamon Press, Oxford.

HORIO, M. & NONAKA, A. 1987 A generalized bubble diameter correlation for gas–solid fluidized beds. *AIChE Jl* **33,** 1865–1872.

HORIO, M. & MORISHITA, K. 1988 Flow regimes of high velocity fluidization. *Jap. J. Multiphase Flow* **2,** 117–136.

HORIO, M., ISHII, H., KOBUKAI, Y. & YAMANISHI, N. 1989 A scaling law for circulating fluidized beds. *J. Chem. Engng Japan* **22,** 587–592.

HORIO, M., ISHII, H. & NISHIMURO, M. 1992 On the nature of turbulent and fast fluidized beds. *Powder Technol.* **70,** 229–236.

ISHII, H. & MURAKAMI, M. 1991 Evaluation of the scaling law of circulating fluidized beds in regard to cluster behaviors. In *Circulating Fluidized Bed Technology III* (Edited by BASU, P. *et al.*), pp. 125–130. Pergamon Press, Oxford.

LANNEAU, K. P. 1960 Gas–solid contacting in fluidized beds. *Trans. Inst. Chem. Engng* **38,** 128.

TSUKADA, M., NAKANISHI, D., TAKEI, Y., ISHII, H. & HORIO, M. 1991 Hydrodynamic similarity of a circulating fluidized bed under different pressure conditions. In *Proc. 11th Int. Conf. on Fluidized Bed Combustion* (Edited by ANTHONY, E. J.), pp. 829–834. ASME, New York.

WEIMER, A. W. & JACOB, K. V. 1986 On bed voidage and apparent dilute phase hold-up in high pressure-turbulent fluidized beds of fine powders. In *Fluidization V* (Edited by OSTERGAARD, K. & SORENSEN, A.), pp. 313–320. Engineering Foundation, New York.

WEN, C. Y. & YU, Y. H. 1966 A generalized method for predicting the minimum fluidization velocity. *AIChE Jl* **12,** 610.

YANG, C. V. & CHITESTER, D. C. 1988 Transition between bubbling and turbulent fluidization at elevated pressure. *AIChE Symp. Ser.* **262**(84), 10–21.

YERUSHALMI, J. & CANKURT, N. T. 1979 Further studies of the regimes of fluidization. *Powder Technol.* **24,** 187–205.